

VUV properties of Eu-doped alkaline earth magnesium silicate

Akira Komeno^a, Kazuyoshi Uematsu^b, Kenji Toda^{a,*}, Mineo Sato^b

^a Graduate School of Science and Technology, Niigata University, Japan

^b Faculty of Engineering, Niigata University, Japan

Received 2 August 2004; received in revised form 26 December 2004; accepted 13 January 2005

Available online 18 July 2005

Abstract

Plasma display panels (PDP) are most promising for large flat panel displays at present. However, luminescence efficiency and lifetime of PDP phosphors should be improved. Alkaline earth silicates show remarkable properties as phosphor hosts with various crystal structures and high chemical stability. Availability of $\text{Ba}_2\text{MgSi}_2\text{O}_7$ has received attention as a host for vacuum ultraviolet (VUV) excitable phosphor. Blue-green phosphor $\text{Ba}_2\text{MgSi}_2\text{O}_7:\text{Eu}^{2+}$ with a high thermal quenching temperature [G. Blasse, W.L. Wanmaker, J.W. ter Vrugt, A. Brill, Philips. Res. Rep. 23 (1968) 189–200] exhibit high luminance (45% of commercial green VUV phosphor $\text{Zn}_2\text{SiO}_4:\text{Mn}^{2+}$) under VUV excitation without optimization of synthesis condition and emission color. $\text{Ba}_2\text{MgSi}_2\text{O}_7$ is promising candidate for the new VUV phosphor in PDP and mercury-free lamp application.

© 2005 Elsevier B.V. All rights reserved.

Keywords: Vacuum ultraviolet; Silicate; Akermanite; Plasma display panel

1. Introduction

Luminescence centers of phosphors in PDP are excited by host absorption of high VUV energy. Therefore, selection of host with high VUV energy absorbability is important to obtain the high luminance under VUV excitation. Silicate phosphors are promising as candidates of host materials for the new VUV phosphors with various crystal structures and high chemical stability. The emission wavelength of Eu^{2+} depends strongly on the surrounding environments of the Eu^{2+} ion. Alkaline earth silicates emit various color photoluminescence according to the various crystal fields [2–4]. Numerous researchers have examined the luminescence properties of alkaline earth magnesium silicates, $\text{Sr}_3\text{MgSi}_2\text{O}_8:\text{Eu}^{2+}$, $\text{Ba}_2\text{MgSi}_2\text{O}_7:\text{Eu}^{2+}$ [5], $\text{MSiO}_4:\text{Eu}^{2+}$, Eu^{3+} (M = Ca, Sr and Ba) [3], $\text{Ca}_2\text{MgSi}_2\text{O}_7:\text{Eu}^{2+}$ [6], $\text{M}_2\text{MgSi}_2\text{O}_7:\text{Eu}^{2+}$, Dy^{3+} (M = Ca, Sr and Ba) [7],

MMgSiO_4 (M = Ca, Sr and Ba) [8] and MMgSi_2O_8 (M = Ca, Sr and Ba) [9]. Kunimoto et al. reported an excellent VUV luminescence property of $\text{CaMgSi}_2\text{O}_6:\text{Eu}^{2+}$ as VUV phosphor [10]. The Ca site in $\text{CaMgSi}_2\text{O}_6:\text{Eu}^{2+}$ is coordinated by eight oxide ions of Si_2O_6 and MgO_6 units. Alkaline earth ion site in layer structure $\text{M}_2\text{MgSi}_2\text{O}_7$ (M = Ca and Sr) is also coordinated with eight oxide ions of $[\text{MgO}_4]$ and $[\text{SiO}_4]$ units. The thermal quenching temperature of $\text{Ba}_2\text{MgSi}_2\text{O}_7$ is higher than that of $\text{Ca}_2\text{MgSi}_2\text{O}_7$ and $\text{Sr}_2\text{MgSi}_2\text{O}_7$ [1]. Therefore, $\text{Ba}_2\text{MgSi}_2\text{O}_7$ is a candidate as a host for a new VUV phosphor. However, the crystal structure of $\text{Ba}_2\text{MgSi}_2\text{O}_7:\text{Eu}^{2+}$ has not been reported up to now.

Herein, we report the crystal structure and VUV luminescence property of $\text{Ba}_2\text{MgSi}_2\text{O}_7:\text{Eu}^{2+}$ as the new VUV phosphor.

2. Experimental

Phosphors were synthesized using solid-state reaction method. High purity BaCO_3 , MgO , SiO_2 and Eu_2O_3 were employed as raw materials. Appropriate amounts of raw

* Corresponding author. Present address: Department of Chemistry and Chemical Engineering, Faculty of Engineering, Niigata University, 8050 Ikarashi 2-nocho, Niigata 950-2181, Japan. Tel.: +81 25 262 6771; fax: +81 25 262 6771.

E-mail address: f03k111a@mail.cc.niigata-u.ac.jp (K. Toda).

materials were mixed by ball milling using the ZrO_2 ball (5 mm diameter) for 4 h. Samples were prepared by firing at 1473 K for 6 h in air. Then the fired samples were reheated at 1473 K for 6 h in a reductive atmosphere of 5% H_2 –95% Ar gas. Powder XRD data were obtained using a diffractometer (MX-Labo; Mac Science Ltd.). Crystal structure refinement was carried out using the Rietveld method [11] with the Rietan 2000 profile refinement program [12]. The relative luminance of the phosphors under VUV excitation (lamp: UER20H-146VA; Ushio Inc.) was recorded using a luminance colorimeter (BM-7; Topcon Corp.).

3. Results and discussion

Shimizu et al. reported that the crystal structure of $Ba_2MgSi_2O_7$ was the tetragonal akermanite-type structure with the space group $P\bar{4}2_1m$ (No. 113) from single crystal X-ray investigation [13]. The Eu^{2+} doped sample $Ba_2MgSi_2O_7:Eu^{2+}$ was melted at 1573 K: the powder sample was synthesized at 1473 K. The powder XRD pattern of $Ba_2MgSi_2O_7:Eu^{2+}$ (5 mol%) differs from that of single crystal $Ba_2MgSi_2O_7$. A comparison between the powder and single crystal XRD patterns is shown in Fig. 1. The crystal structures of $Ba_2MgSi_2O_7:Eu^{2+}$ were not attributable to the tetragonal symmetry. Indexing of the XRD pattern for the powder sample, $Ba_2MgSi_2O_7:Eu^{2+}$ has monoclinic symmetry, $C2/c$ (No. 15), with the lattice parameters $a = 0.8426$ nm, $b = 1.0726$ nm, $c = 0.8449$ nm and $\beta = 110.763^\circ$. From the combination of indexing and Fourier analysis, a starting model for the crystal structure refinement adopted a structure of distorted monoclinic $Ba_2CoSi_2O_7$ [14]. Refined crystallographic parameters of the powder samples were: $a = 0.8428$ (3) nm, $b = 1.0729$ (3) nm, $c = 0.8452$ (3) nm and $\beta = 110.755$ (3) $^\circ$. Pattern fitting and crystallographic data of $Ba_2MgSi_2O_7:Eu^{2+}$ are shown, respectively, in Fig. 2 and Table 1. Fig. 3 shows that the crystal structure is layered structure with the double Ba^{2+} ion layer between distorted layers consist of $[SiO_4]$ and $[MgO_4]$ tetrahedral. Tetragonal and monoclinic structures have a similarly layered structure aside from their different barium coordinations. It is considered that the synthesis temperature and annealing time are most important factors whether $Ba_2MgSi_2O_7$ take the two-type structure, tetragonal or monoclinic.

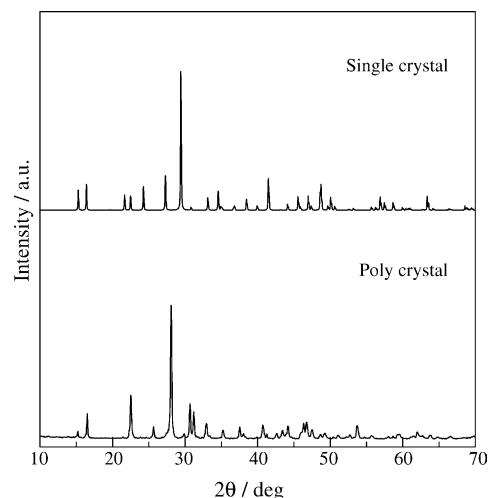


Fig. 1. XRD patterns of the poly crystal $Ba_2MgSi_2O_7:Eu^{2+}$ and simulation $Ba_2MgSi_2O_7$ single crystal.

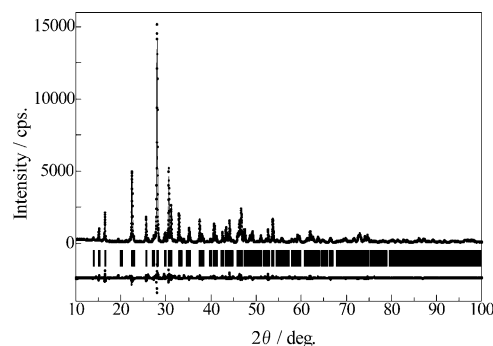


Fig. 2. X-ray pattern fitting for $Ba_2MgSi_2O_7:Eu^{2+}$. The calculated and observed patterns are shown on the top solid line and the dots, respectively. Vertical marks in the middle show positions calculated for Bragg reflections. The bottom trace is a plot of the difference between calculated and observed intensities.

Under VUV (146 nm) excitation, $Ba_2MgSi_2O_7:Eu^{2+}$ showed strong green emission. The critical concentration of Eu^{2+} in $Ba_2MgSi_2O_7:Eu^{2+}$ was 5% under 146 nm excitation. The luminance was 45% of commercial green VUV phosphor $Zn_2SiO_4:Mn^{2+}$ without optimization of the synthetic condition and the emission color. The two reasons are suggested to the high luminance of layered structure,

Table 1

Crystallographic data for $Ba_2MgSi_2O_7:Eu^{2+}$

Atoms	Site	<i>g</i>	<i>x</i>	<i>y</i>	<i>z</i>	<i>B</i> (nm ⁻²)
Ba1/Eu1	8f	0.95/0.05	0.2278 (2)	0.0436 (1)	0.476 (1)	0.0061 (4)
Mg1	4e	1	0.000	0.7438 (1)	0.250	0.0081 (2)
Si1	8f	1	0.1116 (1)	0.2815 (5)	0.1334 (1)	0.0072 (1)
O1	8f	1	0.1002 (1)	0.1440 (1)	0.1187 (2)	0.0150 (3)
O2	8f	1	0.3049 (1)	0.3421 (1)	0.2361 (1)	0.0016 (1)
O3	8f	1	0.4791 (1)	0.1450 (1)	0.0415 (1)	0.0012 (4)
O4	4e	1	0.000	0.3338 (1)	0.250	0.0093 (4)

Space group: $C2/c$ (A-15), crystal system: monoclinic cell constants: $a = 0.8427$ (3) nm, $b = 1.0727$ (3) nm, $c = 0.8451$ (3) nm, $\beta = 110.754$ (2) $^\circ$, $R_{wp} = 11.65\%$, $R_1 = 2.76\%$, $R_F = 1.02\%$ and $S = 1.99$.

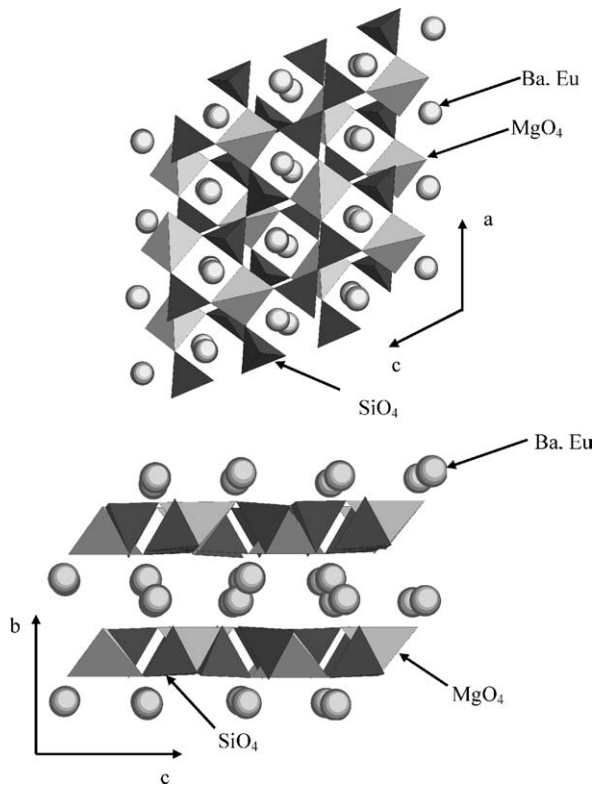


Fig. 3. Crystal structure of $\text{Ba}_2\text{MgSi}_2\text{O}_7:\text{Eu}^{2+}$.

i.e. a two-dimensional structure, $\text{Ba}_2\text{MgSi}_2\text{O}_7:\text{Eu}^{2+}$ with Eu^{2+} ions in the interlayer. First, the critical concentration of emission intensity is very high in $\text{Ba}_2\text{MgSi}_2\text{O}_7:\text{Eu}^{2+}$ because low probability for the excitation energy to be trapped by killer centers in the low dimension a host [15]. Second, this compound has a high thermal quenching temperature because of low thermal vibration by the barium ion's heavy atomic weight [1].

The luminescence wavelength of $\text{Ba}_2\text{MgSi}_2\text{O}_7:\text{Eu}^{2+}$ shifts to the longer wavelength side with the increase of Eu^{2+} concentration. The shift is inferred to be attributable to the crystal field strength. Crystal field influence energy level easily because $4f^65d$ has an electron cloud with large distribution. Splitting of energy level $4f^65d$ become wider with crystal field strength stronger, the difference between ground state 8S level and lower $4f^65d$ component becomes lower. Therefore, the luminescence wavelength shifts to the long wavelength side. The crystal field becomes stronger with increased Eu^{2+} composition because the ionic radius of Eu^{2+} (0.139 nm) is smaller than Ba^{2+} (0.156 nm). The strong crystal field causes the luminescence wavelength shift of $\text{Ba}_2\text{MgSi}_2\text{O}_7:\text{Eu}^{2+}$.

For that reason, the luminescence wavelength shift shorter wavelength side in Eu^{2+} doped akermanite-type host lattice with larger alkaline earth ion.

Although the ionic radius of Ba^{2+} ion is larger and than that of Ca^{2+} ion (small) and Sr^{2+} (middle) ion, the luminescence color of green $\text{Ba}_2\text{MgSi}_2\text{O}_7:\text{Eu}^{2+}$ (504.2 nm)

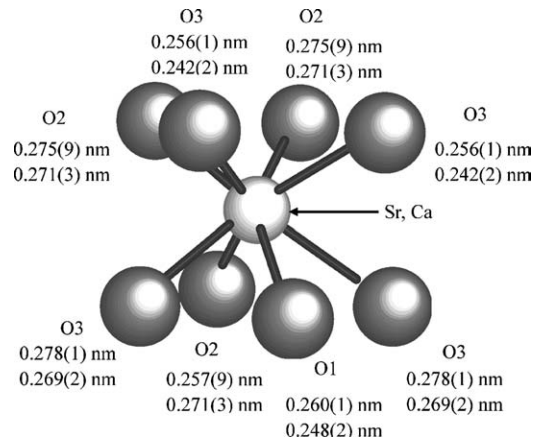


Fig. 4. Coordinated environment of Eu^{2+} in $\text{M}_2\text{MgSi}_2\text{O}_7$ ($\text{M}=\text{Ca}$ and Sr). Upper and lower numbers are distances of $\text{Sr}-\text{O}$ and $\text{Ca}-\text{O}$, respectively.

is between yellow $\text{Ca}_2\text{MgSi}_2\text{O}_7:\text{Eu}^{2+}$ (518 nm) and blue $\text{Sr}_2\text{MgSi}_2\text{O}_7:\text{Eu}^{2+}$ (469 nm). The irregular shift of the luminescence wavelength results from the difference of the crystal structure. The coordination environment of Eu^{2+} in the monoclinic $\text{Ba}_2\text{MgSi}_2\text{O}_7:\text{Eu}^{2+}$ differs from that in tetragonal $\text{Ca}_2\text{MgSi}_2\text{O}_7:\text{Eu}^{2+}$ and $\text{Sr}_2\text{MgSi}_2\text{O}_7:\text{Eu}^{2+}$. The crystal structures of $\text{Ca}_2\text{MgSi}_2\text{O}_7:\text{Eu}^{2+}$ and $\text{Sr}_2\text{MgSi}_2\text{O}_7:\text{Eu}^{2+}$ are isomorphic tetragonal structure ($P\bar{4}2_1m$ No. 113). The coordinated environment of Eu^{2+} in $(\text{Sr}, \text{Ca})_2\text{MgSi}_2\text{O}_7:\text{Eu}^{2+}$ and that of $\text{Ba}_2\text{MgSi}_2\text{O}_7:\text{Eu}^{2+}$ are shown, respectively, in Figs. 4 and 5. Table 2 lists the bond lengths between neighboring oxygen atoms and alkaline earth ionic sites. The Eu^{2+} in $\text{Ca}_2\text{MgSi}_2\text{O}_7:\text{Eu}^{2+}$ and $\text{Sr}_2\text{MgSi}_2\text{O}_7:\text{Eu}^{2+}$ have similar coordination environments. Alkaline earth ion sites in interlayer are coordinated by eight neighboring oxygen ions of each layer and consist of $[\text{SiO}_4]$ and $[\text{MgO}_4]$ tetrahedra. As the ion radius of alkaline earth ion becomes larger in these compounds, the wavelength is shifted to the shorter wavelength side because of the strong crystal field.

On the contrary, the coordination environment of Eu^{2+} in $\text{Ba}_2\text{MgSi}_2\text{O}_7:\text{Eu}^{2+}$ differs greatly from those of $\text{Ca}_2\text{MgSi}_2\text{O}_7:\text{Eu}^{2+}$ and $\text{Sr}_2\text{MgSi}_2\text{O}_7:\text{Eu}^{2+}$, as shown in Figs. 4 and 5. The coordination environment of the alkaline

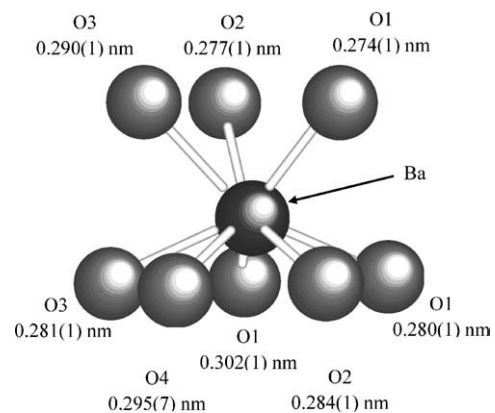


Fig. 5. Coordinated environment of Eu^{2+} in $\text{Ba}_2\text{MgSi}_2\text{O}_7:\text{Eu}^{2+}$.

Table 2

Bond lengths between the alkaline earth ion site and oxygen atoms in $M_2MgSi_2O_7:Eu^{2+}$ (M = Ca, Sr and Ba)

	Average distance (nm)
M = Ba	
Ba–O1	0.274 (1)
Ba–O1	0.280 (1)
Ba–O1	0.302 (1)
Ba–O2	0.277 (1)
Ba–O2	0.284 (1)
Ba–O3	0.281 (1)
Ba–O3	0.290 (1)
Ba–O4	0.295 (7)
M = Sr	
Sr–O1	0.260 (1)
Sr–O2	0.257 (9)
Sr–O2	0.275 (9)
Sr–O2	0.275 (9)
Sr–O3	0.256 (1)
Sr–O3	0.256 (1)
Sr–O3	0.278 (1)
Sr–O3	0.278 (1)
M = Ca	
Ca–O1	0.248 (2)
Ca–O2	0.271 (3)
Ca–O2	0.271 (3)
Ca–O2	0.271 (3)
Ca–O3	0.242 (2)
Ca–O3	0.242 (2)
Ca–O3	0.269 (2)
Ca–O3	0.269 (2)

earth ion sites and silicates layer in $Ba_2MgSi_2O_7:Eu^{2+}$ are much distorted. The numbers of coordinated neighboring oxygen ions are three from one layer and five from another layer in $Ba_2MgSi_2O_7:Eu^{2+}$. The luminescence wavelength shifts to the long wavelength side because of the weak crystal field of the distorted coordination for $Ba_2MgSi_2O_7:Eu^{2+}$.

The chromatic coordinate of $Ba_2MgSi_2O_7:Eu^{2+}$ (0.2159, 0.4838) is slightly blue-green compared with pure NTSC green (0.218, 0.712). The green emission is in the good visibility region. Therefore, improvement of the chromatic coordinate engenders higher luminescence for this $Ba_2MgSi_2O_7:Eu^{2+}$. Improvement of chromatic coordinates can be achieved through substitution of alkaline earth ion sites.

4. Conclusion

We investigated the luminescence properties of $Ba_2MgSi_2O_7:Eu^{2+}$ as the host for new VUV phosphors. The XRD pattern of $Ba_2MgSi_2O_7:Eu^{2+}$ is different from that of a single crystal $Ba_2MgSi_2O_7:Eu^{2+}$ [13]. The polycrystalline sample of $Ba_2MgSi_2O_7:Eu^{2+}$ represents a new distorted akermanite-related structure. $Ba_2MgSi_2O_7:Eu^{2+}$ showed relatively high green emission under vacuum ultraviolet. Therefore, $Ba_2MgSi_2O_7:Eu^{2+}$ is a promising candidate as a new VUV phosphor in future PDP applications.

Acknowledgement

This study was supported by the Science and Technology Agency for Millennium Projects (No. 12317).

References

- [1] G. Blasse, W.L. Wanmaker, J.W. ter Vrugt, A. Bril, Philips. Res. Rep. 23 (1968) 189–200.
- [2] K. Yamazaki, H. Nakabayashi, Y. Kotera, A. Ueno, J. Electrochem. Soc. 133 (1986) 657–660.
- [3] T.L. Barry, J. Electrochem. Soc. 115 (1968) 733–738.
- [4] T.L. Barry, J. Electrochem. Soc. 115 (1968) 1181–1184.
- [5] G. Blasse, W.L. Wanmaker, J.W. ter Vrugt, J. Electrochem. Soc. 115 (1968) 673.
- [6] L. Jiang, C. Chang, D. Mao, C. Feng, Mater. Sci. Eng. B 103 (2003) 271–275.
- [7] Y. Lin, C.W. Nan, X. Zhou, J. Wu, H. Wang, D. Chen, S. Xu, Mater. Chem. Phys. 82 (2003) 806–863.
- [8] Y. Lin, Z. Tang, Z. Zhang, C.W. Nan, J. Alloys Compd. 348 (1–2) (2003) 76–79.
- [9] S.H.M. Poort, H.M. Reijnhoudt, H.O.T. van der Kuip, G. Blasse, J. Alloys Compd. 241 (1996) 75–81.
- [10] T. Kunimoto, R. Yoshimatsu, K. Ohmi, S. Tanaka, H. Kobayashi, IEICE Trans. Electron. 11 (2002) 1888–1894.
- [11] H.M. Rietveld, Acta Crystallogr. 22 (1967) 151.
- [12] F. Izumi, T. Ikeda, Mater. Sci. Forum 198 (2000) 321–324.
- [13] M. Shimizu, M. Kimata, I. Iida, N. Jb. Miner. Mh. H1 (1995) 39–47.
- [14] Y.A. Malinovskii, Dokl. Akad. Nauk SSSR 278 (1984) 616–619.
- [15] H. Yamamoto, Oyobuturi 20 (3) (2000) 309–312 (in Japanese).